A general framework for 3D interpretation of magnetic data affected by remanence and self-demagnetization

Yaoguo Li* and Richard A. Krahenbuhl
Center for Gravity, Electrical & Magnetic Studies (CGEM); Colorado School of Mines

This paper was prepared for presentation during the 12th International Congress of the Brazilian Geophysical Society held in Rio de Janeiro, Brazil, August 15-18, 2011.

Abstract

3D inversion of magnetic data has been successfully used in many aspects of geophysical exploration over the last decade. In a majority of cases, one can assume that the direction of magnetization is the same as the current inducing field direction, and generalized magnetic inversions requiring this information typically perform well in recovering susceptibility distributions. However, the sometimes unknown direction of total magnetization, caused either by the presence of high magnetic susceptibility or remanent magnetization, has limited the use of this technique. We present a general framework for solving these problems by examining the three classes of magnetization and formulate a suite of methods of practical utility in any magnetic environment. The first class performs inversion for the case of induced magnetization with weak magnetic susceptibility, where the magnetization direction is the same as the Earth's inducing field. The second class focuses on the estimation of total magnetization direction when the field is not purely induced, and then incorporates the resultant direction into an inversion algorithm that assumes a known direction. The final class focuses on the direct inversion of the amplitude of magnetic anomaly vector, a quantity that depends weakly upon magnetization direction. With these new developments, we show that it is now feasible to invert any magnetic exploration data set, regardless of whether it is purely induced, or affected by strong remanence or self-demagnetization.

Introduction

Quantitative interpretation of magnetic data through inversion for general distribution of magnetic susceptibility has been playing an increasingly important role in exploration in recent years. Such applications range from local-scale to large-scale problems. Most currently available algorithms require the knowledge of magnetization direction, since it is an essential piece of information for carrying out the forward modeling (e.g., Li and Oldenburg, 1996; Pilkington, 1997). In most cases, one can simply assume that there is no remanent magnetization and the self-demagnetization effect can be neglected. Consequently, the direction of magnetization is assumed to be the same as the current inducing field direction. This is a valid assumption in a majority of cases, as evidenced by many successful applications.

However, there are well-documented cases in which such an assumption is inadequate due to the presence of remanent magnetization or self-demagnetization (e.g., Wallace, 2006). The total magnetization direction can be significantly different from that of the inducing field when remanence is present, or highly varying in space within a highly susceptible geologic unit. Without prior knowledge of the direction of resultant magnetization, current inversion algorithms may become ineffective. This difficulty has limited the application of these algorithms.

In some respect, the difficulties in applying current magnetic inversion algorithms to these two distinct problems are similar in that the magnetization direction inside the causative body is rotated away from the Earth's inducing field – often drastically. However, the similarities stop there. This is because remanent magnetization and self-demagnetization have entirely different origins. Remanent magnetization is the net magnetization present in a material in the absence of an external field (Merrill et al., 1996). Remanent magnetization can occur for any magnetic geologic unit and commonly does not have strong dependence on geometry of the source body. The total magnetization is the vector sum of the remanent and induced components. Self-demagnetization, in contrast, exists when susceptibilities become large and the magnetic field at a location in the source body is significantly affected by the induced magnetization from neighboring domains (Clark & Emerson, 1999). This process is highly dependent upon the source geometry and the resultant magnetization direction can be much more variable within a single body.

To address these issues, researchers have taken several different routes. For example, Paine et al. (2001) transformed magnetic data with remanence into quantities that resemble total-field anomaly but have less dependence on the magnetization direction prior to applying 3D inversions. Lelievre et al. (2006) expanded the standard inversion to recover three components of total magnetization vector. Lelievre and Oldenburg (2006) also formulated a nonlinear magnetic inversion to incoporate the full self-demagnetization solution in the forward mapping.

We have chosen to focus on the magnetization direction as extra parameters in the inversion and developed two interpretation approaches. The first is to estimate the direction of total magnetization and supply it to the inversion algorithm, assuming that the magnetization direction does not vary greatly within the target region. There are a number of approaches for estimating magnetization direction for this approach. As we illustrate in this paper, such an assumption may often prove valid for the remanence problem, however, this assumption breaks down in the presence of strong self-demagnetization with higher magnetic susceptibilities. Alternatively, we accept the fact that a single direction may not be estimated for a particular data set and, therefore, opt to directly invert a quantity that is calculated from magnetic data but is insensitive to magnetization direction. Based on these methods, we have developed a general framework for the interpretation of magnetic data in any environment.

In the following, we illustrate these distinct interpretation approaches applied to 3D magnetic interpretation when first, the anomaly results from induced magnetization; second, when remanent magnetization is present; and finally when self-demagnetization exists. We begin with a brief summary of these methodologies, and then demonstrate their effectiveness and discuss their limitations. For brevity and consistency, we use a synthetic example here for illustration, but will present different case histories in the presentation.

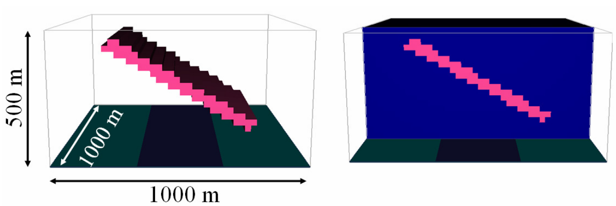

Figure 1: *Tabular shaped body to demonstrate the effectiveness and limitations of various magnetic interpretation techniques when data are the result of induced magnetization, remanent magnetization, and self-demagnetization.*

Methodology

Inversion for induced magnetization

This is the most mature approach with the simplified assumptions that there is no remanent magnetization and the self-demagnetization is negligible. Under these assumptions, the magnetization direction is known to be the same as the inducing field and a simple forward mapping from the subsurface susceptibility model to magnetic data is defined. The basic inversion algorithm consists of a standard application of inverse theory to the problem with the additions of bound constraints and a requisite depth weighting (Li and Oldenburg, 1996). The model region is divided into a set of continuous rectangular prisms each with a constant susceptibility value. Therefore, the 3D distribution of the magnetic susceptibility is represented as a piece-wise constant function. This standard algorithm can be accelerated by the use of wavelet compression of the dense sensitivity matrix (Li and Oldenburg, 2003).

Inversion with estimation of total magnetization direction

When one of the above assumptions is no longer valid, the actual magnetization direction may no longer be known. Thus, we lack a crucial piece of information to carry out the forward mapping in the inversion. A logical approach would be to attempt estimating the direction and then use it in the inversion.

Given the importance of the magnetization direction in the magnetic interpretation, it is not surprising that many authors have published on this subject over the past several decades. For example, Zietz and Anderson (1967) have utilized the relationship between locations of the maximum and minimum of an anomaly produced by an anomalous source body. In 1993, Roest and Pilkington presented us with a method in which they correlated the amplitude of the total gradient of the magnetic field and the horizontal gradient of the pseudogravity. Haney and Li (2002) developed an approach for estimating total magnetization for a 2D data set using wavelets. Lourenco and Morrison (1973) develop a method based upon the integral relationships of magnetic moments derived by Helbig (1962). Similarly, in 2005, Phillips developed an additional method that likewise utilizes the integral relationships derived by Helbig (1962). Dannemiller and Li (2006) implemented a cross-correlation method for estimating magnetization by examining the symmetry of various RTP fields. These are just a few examples of the work that has been done in estimating total magnetization, and each method carries its own strengths and weaknesses.

Once the direction is estimated, it can be input into the standard inversion algorithm and we recover the distribution of the effective susceptibility, which is the ratio of the magnitude of magnetization over the Earth's inducing magnetic field. This method was first developed for the case of remanent magnetization. For data sets with a single anomaly, this method can be very effective. The direction estimation is carried out in the data domain and the associated computational cost is negligible. With a reliable estimation of the magnetization direction, the inversion result can be excellent. However, the difficulty in working with the estimation techniques is that they typically assume the local magnetic field is not perturbed significantly within the causative body and thus the magnetization direction is approximately constant. While this is valid for many remanent magnetization problems, it is commonly violated for problems of high magnetic susceptibility leading to strong self-demagnetization effect.

For our purpose of interpreting magnetic data, we have not observed a distinct advantage of one method over the others for estimating total magnetization direction. For this reason, we demonstrate the relative merits and limitations of providing total magnetization direction to the magnetic inversion algorithm when data are strongly affected by either remanence or self-demagnetization.

Amplitude inversion

Nabighian (1972) showed that the amplitude of an anomalous magnetic field, or the total gradient of the magnetic anomaly vector, is independent of the magnetization direction in 2D problems. While such a property does not extend exactly to 3D problems – because of the absence of a true 3D analytic signal in magnetics – both quantities are only weakly dependent on direction. This is especially true for total gradients when the anomaly has been converted to the vertical component by a half reduction to the pole. This property provides the opportunity for direct inversion of the anomaly amplitude or total gradient to recover the magnitude of magnetization without knowing its direction.

Shearer and Li (2004) developed such an algorithm by formulating a generalized inversion with a positivity constraint on the magnitude of magnetization. The algorithm starts by calculating, for example, the amplitude of the anomalous magnetic field from the observed total-field anomaly. It then treats the amplitude as the input data and recovers the distribution of effective susceptibility as a function of 3D position in the subsurface.

One advantage of the approach is that it is not limited to a single anomaly nor does it require that adjacent anomalies have the same magnetization direction. Therefore the approach is potentially applicable to a wide range of problems where the source distribution is more complicated. Since the amplitude data do not preferentially attenuate lower-wavenumber signal as the total gradient does, we have observed that amplitude is preferable to use in practice. This approach provides a reliable alternative for the interpretation of magnetic data over targets exhibiting strong remanence. Similarly, numerical simulation and applications to field data sets indicate that the method greatly outperforms the technique based on direction estimation for targets exhibiting strong self-demagnetization due to high magnetic susceptibilities.

Example

To demonstrate the effectiveness of the afore-mentioned approaches, we utilize a synthetic example consisting of a thin, tabular shaped dipping body for three separate simulations, each with appropriate magnetic properties. The geometry was chosen for these demonstrations because such tabular shaped structures exhibiting remanence and/or self-demagnetization are well recognized in exploration problems, such as for Banded Iron Formations (e.g., Wallace, 2006). The tabular body, Figure 1, is located within a model region spanning 1000m in both northing and easting, and 500m in depth. The body itself strikes north-south with a strike length of approximately 500m. Dip is to the east, with a dipping angle of approximately 30 degrees. The external field for this study has amplitude of 50,000 nT, inclination of 65 degrees, and declination of -25 degrees. Data are then computed at an observation height of approximately 1.0 meter above ground, centered over the body and spanning a survey area of 2,000m in both northing and easting. The datasets are each contaminated with 5 nT Gaussian noise prior to interpretation.

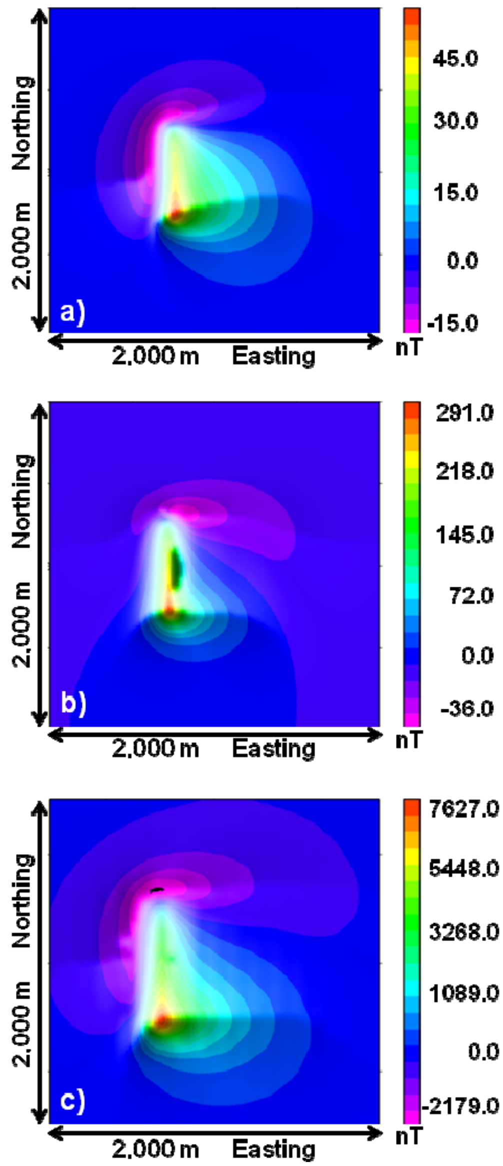

Figure 2: *Magnetic data calculated for the problems of (a) induced magnetization, (b) remanent magnetization, and (c) self-demagnetization. Note the large amplitude of the total-field magnetic data in panel (c), which is often an indication of self-demagnetization.*

<u>Induced magnetization</u>

For the first example, the magnetic susceptibility of the target body is 0.01 SI, and there is no remanent magnetization. With this small susceptibility value, the response is likewise not affected by self-demagnetization effect. We can assume the total magnetization direction is the same as the inducing field direction for inversion. The data are presented in Figure 2(a).

Remanent magnetization

In the second example, we assume the presence of remanent magnetization. In general, we cannot quantitatively distinguish and separate the induced and remanent magnetization components based on the magnetic data alone. Therefore, we adopt a description of the source properties using an effective susceptibility, which is the ratio of magnetization magnitude over the inducing field. In this example, we assume an effective susceptibility of 0.05 and further assume that the presence of remanence caused the total magnetization to be rotated significantly away from the inducing field direction. The data are presented in Figure 2(b), and the difference in the location of the negative peak is distinct in comparison with the data in Figure 2(a). For this example, the resulting total magnetization direction has inclination of 35 degrees and declination of 45 degrees.

Self-demagnetization

The third example is a demonstration of data interpretation for a target with high susceptibility. The dipping body is assigned a magnetic susceptibility value of 3.0 SI. We note that most geologic problems do not contain susceptibility values greater than $\kappa \sim 3$SI. For this example, the self-demagnetization effect is calculated for the discretized susceptibility model subject to the uniform external field. The solution is obtained by solving an integral equation involving the three components of the magnetization vector in the cells. The data results are presented in Figure 2(c). For this large susceptibility, the total-magnetization rotates slightly clockwise away from the inducing field and towards the long axes of the tabular body. In response, the measured field is likewise rotated clockwise. Indicative of self-demagnetization effect, the anomalous field is likewise significantly stronger than the purely induced response in Figure 2(a).

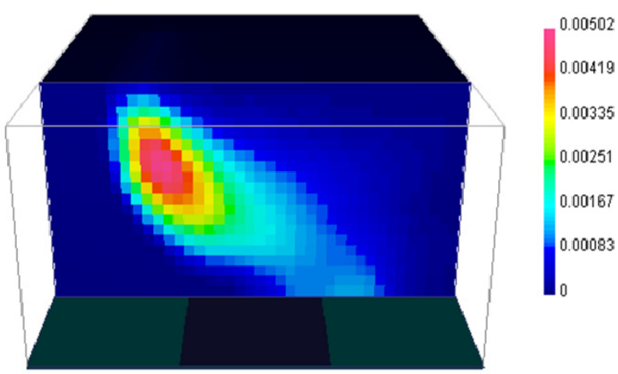

Figure 3: *Standard inversion result for induced magnetization problem with low susceptibility. The approach has nicely captured both the location and dip information of the magnetic dyke. Susceptibility units are in SI.*

Results

In this section, we present and compare inversion results from the above examples to highlight the relative merits and limitations of traditional magnetic inversion, as well as amplitude inversion, when we are faced with either an induced, remanent, or self-demagnetization response.

Induced magnetization

The inversion result for the purely induced problem is presented in Figure 3. For this example with small susceptibility and no remanent magnetization effect, the magnetization direction throughout the dyke model is constant and equal to the inducing field direction. The standard inversion approach, introduced in the first part of the *Methodology* section, has nicely captured both the location and dip information of the magnetic dyke, thus providing an effective interpretation tool for purely induced problems. The advantage to this approach is that, in most exploration cases, the direction of magnetization can in fact be assumed the same as the current inducing field direction, and self-demagnetization can often be ignored. Thus, this approach provides a reliable means of interpreting magnetic data in a majority of magnetic environments.

Remanent magnetization

For the second example, we demonstrate results using the two later approaches described in the *Methodology* section. That is, we first generate an estimate of the total magnetization direction from the magnetic data, and supply this information to the standard inversion algorithm. Second, we calculate the amplitude of the anomalous magnetic field data, and supply this information as input data for amplitude inversion. For the first approach, magnetization direction is estimated based on Helbig's moment method (1962), with an inclination of 21 degrees and declination of 45.5 degrees.

The results for both approaches are illustrated in Figure 4. Each of the techniques has successfully identified similar location for the upper portion of the magnetic body in this example. The result for the first approach (panel a), however, identifies a possible dip direction for the dyke that is reversed from the true dip. While this approach has proven successful for many remanent magnetization problems (ex: Dannemiller and Li, 2006), as we demonstrate here, the final inversion result is ultimately limited by one's ability to estimate magnetization direction.

Amplitude inversion results (panel b) successfully identify both location and dip direction of the magnetic source body for the remanent magnetization problem. It is not always the case that this technique outperforms the previous approach. However, in this example, the technique clearly provides greater insight into the source geometry, thus demonstrating an additional tool for interpreting magnetic data that are strongly affected by remanent magnetization.

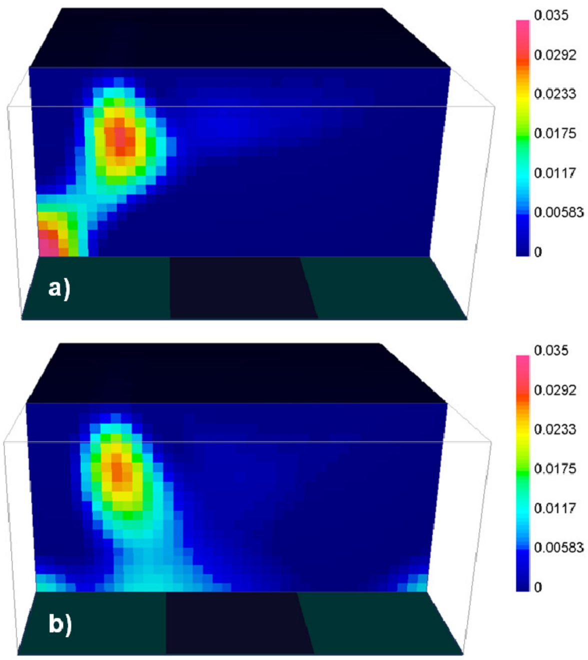

Figure 4: *Remanent magnetization inversion results. The top panel (a) is the result of 3D magnetic inversion when estimated total magnetization direction is supplied to the algorithm. The bottom image (b) is the result from amplitude inversion.*

<u>Self-demagnetization</u>

Similar to the previous example, we present two results for interpretation of the self-demagnetization problem using the same approaches. The first inversion result is recovered by supplying total magnetization direction to the standard inversion algorithm. For illustrative purposes, we have opted to supply the true total magnetization direction to the inversion algorithm here and analyze the performance of the first approach under ideal conditions. For the second approach, we again calculate the amplitude of the anomalous magnetic field data, this time for the self-demagnetization problem, and supply this information as input data for amplitude inversion.

Results from this first approach are presented in Figure 5(a). The recovered model indicates that traditional inversion does not perform well, by any measure, in the presence of strong self-demagnetization. The technique has generated a solution that has a rough structure, poor spatial resolution, and little indication of dip. A similar observation has likewise been observed by Lelièvre and Oldenburg (2006) in which the authors provide an additional method of inverting for high susceptibility using full solution to Maxwell's equations. Results similar to Figure 5(a) will occur using standard inversion, even when knowledge of true total magnetization direction is supplied, and it is the result of highly varying magnetization throughout the source body, in both direction and magnitude, when high susceptibility is present. A single value estimation of magnetization direction is no longer meaningful when self-demagnetization effects are present. While this approach can demonstrated successful for the remanent magnetization problem when an accurate estimation of magnetization direction is identified, the same cannot be said for self-demagnetization application.

In contrast, results from amplitude inversion are presented in Figure 5(b), and it clearly provide greater insight into the location and geometry of the magnetic source body. In this instance, the depth and location of the top of dyke is well recovered, and we have likewise constructed a smooth, compact body that adequately approximates dip of the original tabular structure. Thus, the method of amplitude inversion is clearly preferred for 3D interpretation of magnetic data when there is high susceptibility and strong self-demagnetization effect.

Discussion

We have presented a general framework for tackling the problem of inverting any magnetic exploration data set, regardless of whether it is purely induced, or affected by strong remanence or self-demagnetization. The approach for addressing these problems begins by examining the three classes of magnetization, and then formulates a suite of interpretation methods for practical utility in any magnetic environment.

The first method performs inversion for the case of induced magnetization with weak magnetic susceptibility, where the magnetization direction is the same as the Earth's inducing field. The second method focuses on the estimation of total magnetization direction when the field is not purely induced, and incorporates the resultant direction into the standard inversion algorithm that assumes a known direction. The final method circumvents the need for reliable knowledge of magnetization direction and, instead, inverts directly the amplitude of the anomalous field to recover the magnitude of the magnetization.

For a given data set, the first question to be answered is whether the data are affected by strong remanent magnetization or self-demagnetization that is not aligned with the current inducing field. If the answer is no, then any standard inversion algorithms for 3D magnetic inversion can be applied. If the answer is yes, the data set should be inverted by using one of the above two approaches depending on the complexity of the magnetic anomaly. The criterion for choosing which method to use is whether a single magnetization direction is a valid assumption and can be estimated. If the answer is yes, then the method based on direction estimation can be used. In practice, this means that only a single compact anomaly is present, although rare cases of multiple anomalies with the same magnetization direction may exist. When the answer is no, then the method of amplitude-data inversion should be used. Such cases include a single anomaly produced by a complex source body or multiple anomalies with different orientations.

It is noteworthy that both methods can effectively construct the source distribution for a compact source body that meets the assumption of a constant magnetization direction. However, when multiple source bodies are present with varying magnetization directions, or when data are strongly affected by self-demagnetization, the amplitude-data inversion proves to be much more versatile. The price we pay for that ability is of course the missing phase information in the data. As a result, the dip of the recovered source distribution may not be clearly imaged.

Given the approaches presented here, we now have a set of tools at our disposal for interpreting magnetic data in the presence of strong remanence and self-demagnetization. Coupled with existing 3D inversion algorithms for induced magnetization, it is now feasible to interpret quantitatively the majority, if not all magnetic data acquired in exploration problems, by constructing 3D distributions of either magnetic susceptibility or the magnitude of magnetization.

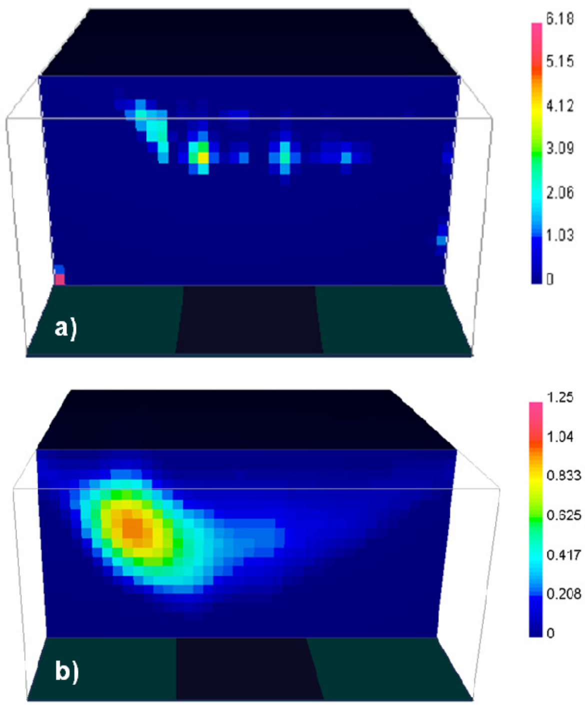

Figure 5: *Self-demagnetization inversion results. The top panel (a) is the result when total magnetization direction is supplied to the standard inversion algorithm. The bottom image (b) is the result from amplitude inversion.*

Acknowledgments

This work was supported by the industry consortium "Gravity and Magnetics Research Consortium" at the Colorado School of Mines. The sponsoring companies are Vale, Petrobras, Marathon, ConocoPhillips, Anadarko, BGP, Fugro, and BP.

References

Clark, D.A., and Emerson, D.W., 1999, Self-demagnetization, Preview (Australian Society of Exploration Geophysicists), Apr/May, 22-25.

Dannemiller, N., and Li, Y., 2006, A new method for estimation of magnetization direction, Geophysics, 71, L69-L73

Haney, M., and Li, Y., 2002, Total magnetization direction and dip from multiscale edges, Expanded Abstracts, 72nd Ann. Internat. Mtg., Soc. Expl. Geophys., Expanded Abstracts

Helbig, K., 1962, Some integrals of magnetic anomalies and their relationship to the parameters of the disturbing body, Zeitschrift Fur Geophysik, 29, 83-97.

Lelievre, P.G., and Oldenburg, D.W., 2006, Magnetic forward modeling and inversion for high susceptibility, Geophysical Journal International, 166, 76-90.

Lelievre, P. G., Oldenburg, D. W., and Phillips, N., 2006, 3D magnetic inversion for total magnetization in areas with complicated remanence, 74th Ann. Internat. Mtg., Soc. Expl. Geophys., Expanded Abstracts

Li, Y., and Oldenburg, D.W., 1996, 3-D inversion of magnetic data: Geophysics, 61, 394-408.

Li, Y., and Oldenburg, D.W., 2003, Fast inversion of large-scale magnetic data using wavelet transforms and a logarithmic barrier method: Geophy. J. Int. 152, 251–265

Lourenco, J. S., and H. F. Morrison, 1973, Vector magnetic anomalies derived from measurements of a single component of the field: Geophysics, 38, 359-368.

Merrill, R.T., McElhinney, M.W., and McFadden, P.L., 1996, The magnetic field of the earth: paleomagnetism, the core, and the deep mantle: Academic Press, Inc.

Nabighian, M., 1972, The analytic signal of two-dimensional magnetic bodies with polygonal cross-section: its properties and use for automated anomaly interpretation: Geophysics, 37, 507-517.

Paine, J., Haederle, M., and Flis, M., 2001, Using transformed TMI data to invert forremanently magnetised bodies: Exploration Geophysics, 32, 238-242.

Phillips, J.D., 2005, Can we estimate total magnetization directions from aeromagnetic data using Helbig's formulas: Earth Planets Space, 57, 681-689.

Pilkington, M., 1997, 3-D magnetic imaging using conjugate gradients, Geophysics, 62, 1132–1142

Roest, W., and M. Pilkington, 1993, Identifying remanent magnetization effects in magnetic data: Geophysics, 58, 653-659.

Shearer, S., and Li., Y., 2004, 3D Inversion of magnetic total-gradient data in the presence of remanent magnetization, 74th Ann. Internat. Mtg., Soc. Expl. Geophys., Expanded Abstracts

Wallace, Y., 2006, 3D modeling of banded iron formation incorporating demagnetization – A case study at the Musselwhite Mine, Ontario, Canada. AESC 2006, Melbourne, Australia.

Zietz, I., and G. E. Andreasen, 1967, Remanent magnetization and aeromagnetic interpretation: Mining Geophysics, 2, 569-590.